HHS Public Access

Author manuscript

Bioconjug Chem. Author manuscript; available in PMC 2022 February 01.

Published in final edited form as:

Bioconjug Chem. 2016 January 20; 27(1): 102–109. doi:10.1021/acs.bioconjchem.5b00524.

Colloidal Confinement of Polyphosphate on Gold Nanoparticles Robustly Activates the Contact Pathway of Blood Coagulation

Magdalena Szymusiak[§,1], **Alexander J. Donovan**[§,1], **Stephanie A. Smith**[2], **Ross Ransom**[1], **Hao Shen**[1], **Joseph Kalkowski**[1], **James H. Morrissey**[2], **Ying Liu**[*,1,3]

[1]Department of Chemical Engineering, University of Illinois at Chicago, Chicago, IL 60607, United States

[2]Department of Biochemistry, University of Illinois at Urbana-Champaign, Urbana, IL 61801, United States

[3]Department of Biopharmaceutical Sciences, University of Illinois at Chicago, Chicago, IL 60607, United States

Abstract

Platelet-sized polyphosphate (polyP) was functionalized on the surface of gold nanoparticles (GNPs) via a facile conjugation scheme entailing EDAC (N-(3-Dimethylaminopropyl)-*N*′-ethylcarbodiimide hydrochloride)-catalyzed phosphoramidation of the terminal phosphate of polyP to cystamine. Subsequent reduction of the disulfide moiety allowed for anchoring to the colloidal surface. The ability of the synthesized polyP-GNPs to initiate the contact pathway of clotting in human pooled normal plasma (PNP) was then assayed by quantifying changes in viscous, mechanical, and optical properties upon coagulation. It is revealed that the polyP-GNPs are markedly superior contact activators compared to molecularly dissolved, platelet-sized polyP (of equivalent polymer chain length). Moreover, the particles' capacity to mobilize Factor XII (FXII) and its co-activating proteins appear to be identical to very-long chain polyP typically found in bacteria. These data imply that nanolocalization of anionic procoagulants on colloidal surfaces, achieved through covalent anchoring, may yield a robust contact surface with the ability to sufficiently cluster active clotting factors together above their threshold concentrations to cease bleeding. The polyP-GNPs therefore serve as a promising foundation in the development of a nanoparticle hemostat to treat a range of hemorrhagic scenarios.

[*]**Corresponding Author** Address: Department of Chemical Engineering, University of Illinois at Chicago, Rm. 211, 810 S. Clinton St., Chicago IL, 60607, United States liuying@uic.edu Tel: (312) 996-8249 Fax: (312) 996-0808.

[§]Equivalent first authors

Author Contributions

M.S., A.J.D., S.A.S., R.R., H.S., and J.K. conceived and conducted experiments. M.S., A.J.D., S.A.S., R.R., H.S., J.K., J.H.M., and Y.L. interpreted the results. M.S., A.J.D., Y.L. and S.A.S. composed the manuscript, with editorial contributions from J.H.M. All authors have given consent to the final version of the manuscript.

Supporting Information Available: *Centrifugation Optimization*. **Supporting Figures:** *Control centrifugation experiments for 10nm GNPs, Control absorbance experiments, Clotting of 50nm polyP*$_{70}$*-GNPs as a function of surface coverage.* This material is available free of charge via the Internet at http://pubs.acs.org.

Conflict of Interest Disclosure

J.H.M. and S.A.S. are co-inventors on patents and pending patent applications related to therapeutic usage of polyP. Y.L. and A.J.D. are co-inventors on a pending patent application associated with the pharmacologic application of polyP nanoparticles. The remaining authors declare no competing financial interests.

Graphical Abstract

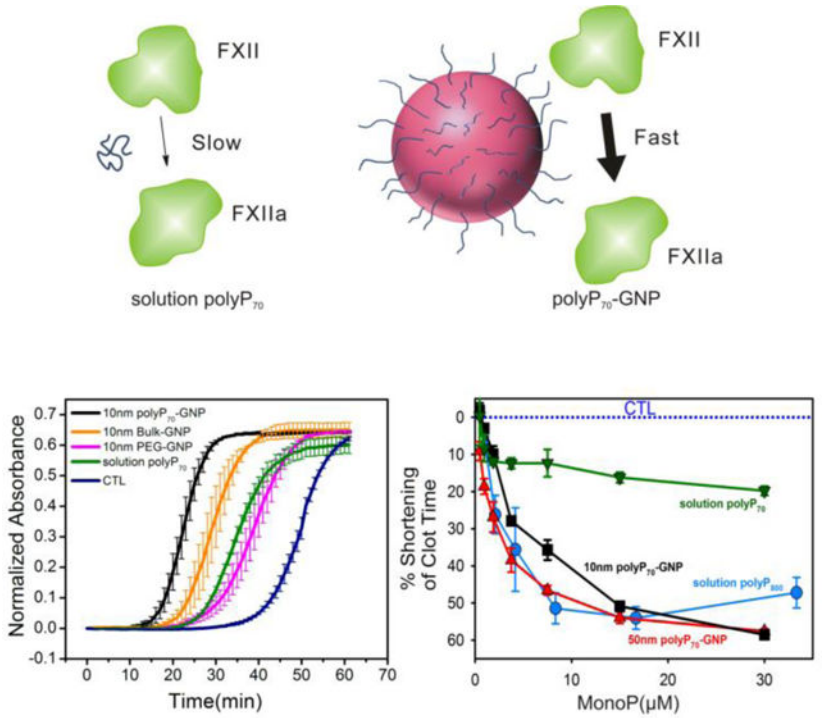

Keywords

polyphosphate (polyP); gold nanoparticle (GNP); *N*-(3-Dimethylaminopropyl)-*N*′-ethylcarbodiimide hydrochloride (EDAC); Factor XII (FXII); Factor XI (FXI); pooled normal plasma (PNP)

Introduction

Polyphosphate (polyP) is an inorganic linear macromolecule consisting of orthophosphates connected by phosphoanhydride bonds.[1] The prevailing thought in the biochemistry community for decades contended that polyP was an early evolutionary casualty in nature's endeavor to design information-dense, multifunctional biomacromolecules.[2] Arthur Kornberg and others[3] in the last two decades have reasserted polyP's significant role in a multitude of organismal processes blurring across taxonomic boundaries: the polymer possesses potent hemostatic, inflammatory, and thrombotic properties,[4–7] hinders tumor growth and angiogenesis,[8] modulates bacterial pathogenicity,[9] chelates toxic metals,[10] aids in DNA transport,[11] and directs histological differentiation,[12, 13] among innumerable other functions. PolyP arguably performs its variegated cellular duties, even with its simple polyphosphoanhydride chemistry, by adopting different macrostructures depending on polymer length, local environment and incoming stimuli similar (but perhaps on a much more rudimentary level) to the plethora of possible tertiary structures encountered with polypeptides. Some prokaryotes surface-pattern long-chain polyPs at varying surface densities on their exterior, with the polymer projecting outward from the cell membrane

into their surroundings. For example, the human infectious agents *N. meningitditis* and *N. gonorrhoeae*, responsible for bacterial meninigitis and gonnorhea, respectively, derive their resilience and virulence in large part from storing a significant fraction of their inorganic phosphate as high-molecular weight polyP on their capsules.[14] The intensely anionic charge density on the exterior is hypothesized to confer protection from a myriad of environmental insults. DoCampo and coworkers discovered condensed polyP on the nanometer-scale in several protozoan species known to infect insects, notably *T. cruzi* and *T. brucei,* in spherical, mildly acidic organelles called acidocalcisomes,[15] colocalized with concentrations of metal ions at levels orders of magnitude higher than in the cytosol. More recently, short-chain polyP has been found in nearly identical subcellular compartments called dense granules in human platelets.[16] We recently established that polyP spontaneously self-assembles into granular nanoparticles in aqueous media containing concentrations of divalent metal cations such as Ca^{2+} and Mg^{2+}, at levels normally found in human blood plasma.[17] The nanoprecipitation is a thermodynamic process governed by the polyP polymer size and the metal ion concentration, with the salt concentration controlling the nanoparticle diameter regardless of polymer supersaturation ratio.[17]

Considerable effort in recent years has centered on implementing novel conjugation chemistries for modifying polyP with various moieties, e.g. fluorescent dyes, biotin, chromogenic substrates, or primary amines, and attaching the polymer to solid substrates for facilitating *in vitro* and *in vivo* detection, quantitating interactions with various binding partners like thrombin, Factor XIIa (FXIIa), Factor XIa (FXIa), and kallikrein, and preventing or slowing enzymatic degradation.[18, 19] Phosphoramidation of the terminal phosphates does not abrogate polyP's physiological functionality, and polyP attached to solid supports retains robust procoagulant ability.[18]

The fact that polyP can exist in a variety of physical manifestations, be it molecularly dissolved, surface-immobilized, granular, or even supported on a colloidal particle scaffold, suggests that these forms might manifest differential procoagulant properties. The varied ability of inorganic polyP to initiate the contact pathway of blood coagulation could be interpreted to substantiate this hypothesis. It has been previously demonstrated that polyP exerts differential clotting effects as a function of polymer length,[6] with high molecular-weight polymers serving as powerful activators of the contact pathway, while intermediate and platelet-sized polyP are less potent contact activators. These shorter polymers are procoagulant through mechanisms impacting enzymes and inhibitors of other portions of the coagulation cascade.[4, 7] It has been shown that negatively charged surfaces are necessary to initiate the contact pathway of blood coagulation.[20] Foreign colloidal particles like ellagic acid[21] and silicate minerals[22] and highly anionic polymers of sufficient molecular weight like sulfated polysaccharides[23] present the FXII zymogen and its enzymatic binding partners (i.e. high molecular weight kininogen (HMWK) and prekallikrein) a sufficiently large nanosurface to trigger clotting. Sulfated polysaccharides such as heparin are generally considered powerful anticoagulants because of binding to antithrombin; however, in the absence of this enzyme inhibitor, we have previously demonstrated that heparin in actuality is a robust procoagulant molecule in many respects similar to polyP.[24] FXII has a molecular weight of 80,000 Da,[25] so its radius of gyration would be ~2–5 nm. As such, long-chain polyP should possess significant ability to activate the contact pathway due its

high molecular weight and large surface area, with both the molecularly dissolved and nanoprecipitated forms arguably being large enough to activate FXII. On the other hand, the ability of molecularly dissolved, short-chain polyP to initiate the contact pathway is a matter of some dispute.[26–28] Recent work by Mutch and colleagues provides evidence that platelet-sized polyP autoactivates FXII *in vitro*, with activity catalyzed by the presence of zinc cations.[29]

In the present investigation we demonstrate that polyP of approximately the size released from platelets conjugated to colloidal gold nanoparticles (GNPs) via phosphoramidate linkages is able to robustly activate the contact pathway of coagulation, with potency equivalent to that of molecularly dissolved, long-chain polyP like that predominately found in bacteria. With further functionalization, polyP-GNP conjugates may be potentially used for targeted delivery as procoagulant agents to the bleeding site, especially benefiting the first-aid treatment of internal hemorrhage. As polyP is already secreted upon platelet activation and naturally exists in the human body, it is anticipated that the introduction of a colloidally-anchored polyP drug delivery vehicle would have minimal side effects compared to other foreign procoagulants. In order to achieve hemostasis, polyP concentrations typically approach the micromolar range in near vascular injury sites and could potentially be much higher within a platelet-dense thrombus.[6] PolyP-GNPs could potentially be of use in the management of bleeding episodes and provide further corroboration that polyP is able to wield its divergent effects by manifesting in a myriad of macrostructural forms.

Results and Discussion

Binding of $polyP_{70}$ to GNPs was achieved by two-stage reaction: (1) $PolyP_{70}$ was first allowed to react with cystamine; (2) The $polyP_{70}$-cystamine conjugate was then reacted with GNPs by replacing the citrate groups (Figure 1).

The primary amine-containing compounds like polyethylenimine, amine-PEG_2-biotin, and spermidine were used previously to study the covalent attachment of primary amine groups with the terminal phosphates of polyP via EDAC-mediated reaction.[18] We modified this method for the coupling of $polyP_{70}$ with cystamine – a disulfide molecule, containing two primary amine groups. Reduction of the disulfide moiety in cystamine then allowed for the attachment to the GNP surface. Reaction conditions (including temperature, reaction time, pH, and buffering environment) were optimized to control the coupling of $polyP_{70}$ with cystamine. For the optimal conditions, $polyP_{70}$ was allowed to react with cystamine at room temperature and pH around 8 for 48 to 72 h. Higher temperature (37 °C) did not improve the yield. A fluorescamine assay was used to test the amount of the unreacted primary amines on cystamine, which indicated the conjugation efficiency. The highest yield of the reaction was approximately 90% as seen in Table 1.

An investigation of P-N bond hydrolysis was carried out to test the stability of the $polyP_{70}$-cystamine ligand. After 72 h of reaction, a fluorescamine assay was performed to detect the concentration of the unreacted cystamine. The samples were monitored for two weeks and hydrolysis of the P-N bonds was quantified. The P-N bond hydrolyzed in acidic conditions

at pH 6.02. It was stable at pH above 7 as presented in Table 2 below. These results were in good agreement with other literature data on P-N bond hydrolysis. [30–34]

The $polyP_{70}$-cystamine conjugate was allowed to react with GNPs of two different sizes (10nm and 50nm) by displacing the citrate group. After 24 h of reaction, salt addition was initiated to increase free GNP surface area available for $polyP_{70}$ attachment. [35] The slow increase in salt concentration in the reaction over a period of four days (0.1 M NaCl final concentration) allowed the already attached $polyP_{70}$ to extend, creating more space for the unreacted ligands to access the gold surface, thus resulting in an increase in the number of $polyP_{70}$ chains per particle. The reaction conditions were modified from the conditions used to conjugate DNA on the surface of gold nanoparticles[35] and their detailed description is presented in the Experimental Procedures. The full coverage is estimated from the theoretical calculations based on the ideal maximum ligand density of 0.22 per square nanometer[36, 37] and found to be 69 and 1727 for 10nm and 50nm GNPs, respectively. The maximized conjugation efficiencies were found to be 24.7% and 46.0% for 10 nm and 50 nm GNPs respectively, comparing the number of conjugated ligands with the theoretical maxima.

Removal of excess, unreacted $polyP_{70}$ left in the solution was achieved via centrifugation. The detailed description of the centrifugation conditions and the centrifugation optimization experiments is provided in the Experimental Procedures and Supporting Information section. After each centrifugation, the supernatant was removed and the pellets were re-suspended with a buffer at pH 7.2 to ensure the stability of the $polyP_{70}$-cystamine ligand and prevent $polyP_{70}$ hydrolysis.

Morphology and stability of the $polyP_{70}$-GNPs were confirmed by TEM (Figure 2), revealing that the $polyP_{70}$-GNP dispersion is largely free of aggregation, and the morphology of the GNPs is indistinguishable from commercially available citrated gold suspensions, that being spherical and uniformly electron dense. High magnification micrographs of 10nm $polyP_{70}$-GNPs reveal the recognizable atomic lattices of the particles, clearly suggesting that the GNPs are nanocrystals.

After purification using centrifugation, concentrations of $polyP_{70}$ were measured using the malachite green assay and concentrations of GNPs were obtained by UV-vis spectroscopy. The number of $polyP_{70}$ on the surface of GNPs was calculated based on the above measurements. The following $polyP_{70}$-GNPs were synthesized and characterized (Table 3) to investigate their ability to initiate the contact pathway of blood coagulation in a concentration-dependent manner.

$PolyP_{70}$-GNPs markedly reduce the time of coagulation in human plasma when assayed for contact activity using a mechanical coagulometer, a standard technique to measure clotting of both whole blood and plasma (Figure 3). Molecularly dissolved $polyP_{70}$ and $polyP_{800}$ were added as a positive control to citrated pooled normal plasma (PNP) at monoP concentrations ranging from 0–30 μM. Clotting was initiated by adding excess $CaCl_2$. Concentration for $polyP_{70}$-GNPs is given in terms of moles of GNPs (not elemental gold). Reduction in clotting time for $polyP_{70}$-GNPs follows typical kinetics of a surface-modulated

reaction mechanism,[38] suggesting that the polyP$_{70}$-GNPs provide a templating surface for FXII activation. PolyP$_{70}$-cystamine ligands conjugated to GNPs of 10- and 50nm diameter robustly activate the contact pathway of coagulation much more efficiently as compared to polyP$_{70}$ in solution.

The clotting activity of both 10nm and 50nm polyP$_{70}$-GNPs is comparable to that of much longer polyP (polyP$_{800}$) and even greater at monoP concentrations exceeding 20μM. These results raise the question that colloidal confinement of polyP may yield divergent outcomes in complex, nonlinear biological processes such as blood coagulation, where threshold concentrations of activators must be attained before a response is generated. In this instance, chemical conjugation of platelet-sized polyP, itself a mediocre activator of the contact pathway, to an essentially inert colloidal surface, transforms the small polymer into an excellent contact activator comparable to polyP approximately ten times larger. Initiation of the contact pathway almost always necessitates a nanosurface of sufficient negative charge density and cross-sectional area to recruit the FXII zymogen. Subsequently, its fellow contact pathway components high molecular weight kininogen (HWMK) and prekallikrein must come in close proximity to FXII to accelerate and propagate the procoagulant stimulus. Anchoring highly anionic polyP$_{70}$ onto 10nm and 50nm GNPs likely generates such an activating surface for the triad of proteins, whereas short-chain polymers that are molecularly dissolved like platelet-sized polyP$_{70}$ do not have adequate radii of gyration to localize FXII, HMWK, and prekallikrein together into the primary complex and propagate the signal. As prekallikrein and HMWK have been found to have a complexed molecular weight of 285 kDa in plasma, a surface larger than 5 nm would most likely be required to properly anchor these proteins together with FXII.[39] Bacterial polyPs, typically several hundred to thousands of orthophosphate residues, have molecular weights and radii of gyration comparable to large globular proteins, suggesting that these polymers are already above this threshold size for anchoring the primary complex, given that they robustly initiate the contact pathway of clotting in a fashion similar to foreign colloidal procoagulant agents.[6] Long-chain polyP with robust contact-pathway activity can accordingly be used as a ruler for the measurement of hemostatic activity of polyP$_{70}$-GNPs and molecularly dissolved polyP$_{70}$ (Figure 3A).

The reduction in clotting time elicited by the polyP$_{70}$-GNPs was further analyzed as a function of the GNP concentration (Figure 3B and C). 50nm polyP$_{70}$-GNPs are more procoagulant, as contrasted with the 10nm polyP$_{70}$-GNPs, at equivalent GNP concentration: the 50nm GNPs reduce the time to clot by 60% at less than 2 nM GNP concentration, whereas it takes approximately 80 nM for the equivalent drop with the 10nm GNPs. This effect can be attributed to the twenty-five fold increase in the surface area of the 50nm GNPs when compared with 10nm GNPs, indicating larger localization of polyP$_{70}$ that could lead to a better recruitment of active clotting factors above their threshold concentration. The curvature of the particles may also affect the structural change of FXII. It is reported by Kushida et al. that nanoparticles of larger size with low curvature effect facilitated higher degree of FXII denaturation, whereas smaller size nanoparticles (high curvature) led to little or no denaturation/unfolding of FXII resulting in much weaker effects on the intrinsic coagulation.[40] Citrated (bulk) and PEGylated GNPs are used as controls to demonstrate that the GNPs themselves are not responsible for the marked reduction in clotting time.

PEGylation of 10nm citrated GNPs after 3–4 days of reaction reveals that the zeta potential drops from −20 to −5 mV, implying that the negatively charged citrate is being replaced by the neutral PEG-thiol (see Table 4). The zeta potential of the synthesized polyP-GNPs is found to be −25mV to −30mV, which is comparable to silica particles with the zeta potential rage form −25mV to −40mV and kaolin suspensions with the zeta potentials ranging from −20mV to −30mV.[41, 42] The silica particles and kaolin have been previously reported to be potent surfaces for contact pathway activation.[43, 44]

The contact activity of the polyP$_{70}$-GNPs was further corroborated by A_{405} turbidity assays in pooled normal plasma (PNP). 10nm and 50nm GNPs have intrinsic absorbance at 405nm; hence, changes in absorbance values must be interpreted cautiously. As the coagulometric assay measures the mechanical and viscous properties of the clotting plasma, the turbidity tests provide complementary information on the optical density of the polymerizing fibrin mesh. Although fibrin clot density is being directly observed, and is a consequence of thrombin kinetics, it is linked to activation of FXII from interaction with a contact surface. Therefore, these two techniques can be used synergistically to evaluate the efficacy of the polyP$_{70}$-GNPs at initiating the contact pathway of clotting.

Before proceeding with the turbidity tests a series of control experiments were performed to ensure that the absorbance of citrated and polyP$_{70}$ conjugated GNPs does not change after incubation in PNP, and that the absorbance detector does not reach a saturating value during or after coagulation. Supporting Figure S2B, C & D demonstrate that the GNPs are colloidally stable in human plasma for at least 1 h, and that A_{405} remains constant. These observations also provide evidence that the GNPs did not aggregate during the clotting assays and that the quantified procoagulant outcomes emerge from the physical parameters we measured in the laboratory. Supporting Figure S2A, E & F show that GNPs at considerably higher concentrations than used in the clotting tests still display a linear relationship with A_{405} turbidity, implying that absorbance values after coagulation will be well below the saturation limit of the detector. Therefore, the absorbance traces can be normalized by subtracting their initial values and directly compared between samples to quantify their procoagulant efficacy. Supporting Figure S2A gives a representative raw absorbance trace of the polyP$_{70}$-GNPs at 5 μM monoP before normalization. The time to initial fibrin formation is typically determined by fitting a line to the point at which the absorbance begins to increase and subsequently finding the intersection with the baseline absorbance value. Figure 4A shows the clotting outcomes (measured by increase in turbidity) of the 10nm polyP$_{70}$-GNPs. PolyP$_{70}$-GNPs manifest a marked increase in turbidity long before polyP$_{70}$ in solution or control with no activator present. Completely PEGylated GNPs likewise do not robustly initiate the contact pathway, with a clotting time between molecularly dissolved polyP$_{70}$ in solution and the control (with no activator present). The citrated 10nm GNPs (bulk), at the same GNP concentration as the 10nm polyP$_{70}$-GNP sample, possess some ability to initiate the contact pathway of clotting, but they are significantly less efficacious than the 10nm polyP$_{70}$-GNPs. Figure 4B depicts the clotting behavior of 10nm and 50nm polyP$_{70}$ -GNPs at 5 μM monoP. All GNPs conjugated with polyP$_{70}$ clot in approximately 10 min, while polyP$_{70}$ in solution coagulates at approximately 25 min, while the control (with no activator present) trails at 35–40 min. The turbidity measurements were all performed at room temperature, and the time to

coagulation will in practice be much longer than those obtained by coagulometry at 37°C. Regardless, the equivalent trends in procoagulant efficacy between samples are apparent after short inspection. These data further corroborate coagulometric measurements presented above that nanoscale confinement of polyP$_{70}$ onto a colloidal surface transforms the weak contact activator polyP$_{70}$ into a robust agent, mimicking polyP chains more than ten times larger.

In the present investigation we lay the groundwork for the implementation of a novel, potentially injectable hemostat for treating a constellation of internal and external hemorrhagic phenomena through the conjugation of platelet-sized polyP to colloidal GNPs, facilitated by phosphoramidation to the disulfide cystamine. Although many negatively charged moieties have been shown to initiate the contact pathway of blood clotting,[45] using polyP has the unique advantages, in that it is naturally secreted by human platelets and in addition to FXII, polyP also interacts with FXI, FV, and thrombin to accelerate clotting. Moreover, our data indicated that the procoagulant effect of polyP conjugated on gold nanoparticles is orders of magnitude greater than any other (as yet) identified anionic polymer. [4, 6, 7] Procoagulant outcomes, measured by conventional contact activity assays in human blood plasma, indicate that they exert significant reductions in the time to clot. Covalent conjugation to the colloidal surface transforms platelet-sized polyP$_{70}$ into a very robust contact surface, similar to that of the potent activator long-chain polyP. These data offer strong support to the claim that clustering of shorter polymers at high local concentrations is equivalent to having much longer polymers dispersed in solution phase for modulation of blood coagulation and other threshold-switchable networks.

The procoagulant activity characteristic of the polyP$_{70}$-GNPs is a meaningful step forward in the development of an on-demand, minimally invasive, targeted hemostat, and surprisingly reminiscent of the threshold-switchable properties of the coagulation cascade itself. Localization of procoagulant activators above crucial threshold concentrations accomplished in physiological contexts allows for swift propagation of the hemostatic signal to achieve wound healing. Organisms have adapted these nonlinear processes capable of exponential amplification, counterbalanced by negative feedback mechanisms, to harbor a rapid response to potentially catastrophic injury, always maintaining this delicate equilibrium of hemostasis essential for survival. The synthesis of polyP$_{70}$-GNPs therefore may fulfill a need for the treatment of a variety of bleeding phenomena, its methodology inspired by nature's nonlinear, threshold-switchable processes.

Experimental Procedures

Materials and reagents—Cystamine, EDAC (*N*-(3-Dimethylaminopropyl)-*N*′-ethylcarbodiimide hydrochloride), MES (2-(N-Morpholino)ethanesulfonic acid), 4-Morpholineethanesulfonic acid), NaCl, MOPS (3-(N-Morpholino)propanesulfonic acid, 4-Morpholinepropanesulfonic acid), imidazole, phosphorus standard solution, ammonium molybdate IV tetrahydrate, malachite green carbinol base, and poly(ethylene) glycol methyl ether thiol (Mn: 1000) were purchased from Sigma Aldrich (St. Louis, Mo, U.S.A.). Colloidal gold citrate nanoparticles (10 and 50 nm-diameter) were purchased from Ted Pella (Redding, CA). PolyP$_{70}$ ('Natrium polyphosphat,' range 20–125 orthophosphates) was

a kind gift from BK Giulini GmbH (Ludwigshafen am Rhein, Germany). PolyP$_{800}$ (range 200–1600) was prepared as previously described.[6]

Synthesis of PolyP$_{70}$-Cystamine Ligand—PolyP$_{70}$-cystamine ligand was conjugated via EDAC mediated reaction.[18] PolyP$_{70}$ (70 mM monophosphate) was added to cystamine (0.1 mM) in the presence of EDAC (300 mM) and MES or MOPS (300 mM) buffers at various pH values (ranging from 6–10) and allowed to mix for 72 h at room temperature (20°C). Control reactions containing all reagents except EDAC were also performed. The efficiency and stability of the reaction at different pH values (ranging from 6–10) were tested by the fluorescamine assay. Briefly, 10 μl of the reaction sample was added to 95 μl of 250 mM borate pH 10, and 45 μl of fluorescamine reagent in acetone (1 mg/ml) in a 96-well black plate. The fluorescamine reagent is known to rapidly bind to the unreacted primary amine group in cystamine, which was measured by using a fluorescence plate reader with excitation wavelength of 365 nm and emission wavelength of 470 nm. A calibration curve was prepared with known concentrations of free cystamine to quantify the amounts of unreacted cystamine in the reaction.

Conjugation of PolyP$_{70}$-Cystamine to GNPs—PolyP$_{70}$-cystamine ligand was allowed to react with GNPs in eight 4 ml reaction vials for 10nm GNPs and eight 2 ml reaction vials for 50nm GNPs. Depending on the nanoparticle size (supplied in different starting particle concentrations or pre-concentrated), the following reagent volumes and concentrations were chosen as indicated in Table 5 below.

Control reactions of PEG-thiol (0.2 mM) with GNPs were also set up. The same reaction volumes were chosen for consistency. The ligands (polyP$_{70}$-cystamine or PEG-thiol) were used in a 2:1 excess ratio to GNP available binding sites. The reaction vials were first kept for 24 h at room temperature with constant slow mixing on a rotator. To increase binding efficiency, the salt addition was initiated to increase the ionic strength of the solution. 10 μl of 5 M NaCl was added to the reaction vials while mixing. The procedure of salt addition was repeated eight times (two times a day with at least a 6 h break in between). The final concentration of salt was 0.1 M NaCl.

Removal of Unreacted PolyP$_{70}$—Unreacted polyP$_{70}$ and ligands were removed by using centrifugation in a Labnet Spectrafuge 16M Microcentrifuge (Labnet International, Woodbridge, NJ). The samples from the polyP$_{70}$-cystamine ligand reactions with GNPs were distributed into 1.6 mL microcentrifuge tubes and centrifuged using optimized conditions (Table 6). After each centrifugation, the supernatant was collected and the GNP pellet was resuspended with the buffer (Imidazole, pH 7.2) by vortexing for 30 s. After final centrifugation for all GNP types, the pellets were resuspended with a smaller amount of buffer in order to achieve desired concentrations of polyP$_{70}$ and GNP.

Determination of Number of PolyP$_{70}$ Chains per Particle—The number of polyP$_{70}$ chains per particle was calculated by quantifying the concentrations of polyP$_{70}$ and GNPs in the concentrated samples after completion of the purification step. To quantify the amount of polyP$_{70}$ present in the sample, 101 μl of sample was mixed with 9.1 μl of 12.1 M HCl and heated at 100 °C for 30 min to first hydrolyze the polyP$_{70}$ chains into monophosphate

(monoP). Then 50 μl of hydrolyzed sample was mixed with 100 μl of malachite green reagent (mixing 0.1% malachite green and 42 mg/ml ammonium molybdate acid solution (5 M HCl) at 3:1 volume ratio) in a 96-well clear plate and allowed to react for 5 min. The amount of monoP present was quantified by measuring the absorbance at 620 nm using a plate reader and comparing the readings with the standardized curve. The amount of GNPs was determined by measuring the absorbance at 405 nm (for 10nm GNPs) and 492 nm wavelengths (for 50nm GNPs) and comparing it with the standard calibration. The final number of $polyP_{70}$ chains per particle was determined by the following formula:

$$Number\ of\ poly\ P_{70}\ chains\ per\ particle\ = \frac{monoP\ concentration\ /\ repeating\ unit}{gold\ nanoparticle\ concentration}$$

Transmission Electron Microscopy (TEM)—$PolyP_{70}$-GNPs or unmodified Au citrate suspension (10 μl) was micropipetted onto a 300-mesh Formvar grid (Structure Probe Inc., West Chester, PA). After 10 min the liquid which had not evaporated was wicked away with the tip of a Kim Wipe®. The samples were examined in a JEM-3010 transmission electron microscope (JEOL Inc., Tokyo, Japan).

Zeta (ζ) Potential Measurements—Zeta potentials of the synthesized $polyP_{70}$-GNPs and PEG-GNPs were measured by using a Zetasizer Nano ZS instrument (Malvern Instruments, Worcestershire, U.K) in DI water at 20 °C.

Clotting Assays—Contact pathway activity of $polyP_{70}$-GNPs was determined by coagulometric assay.[6] Clotting times of citrated human pooled normal plasma (PNP) (George King Biomedical, Overland Park, KS) were quantified at 37°C using a Start 4 coagulometer (Diagnostica Stago, France). Prewarmed polyP or $polyP_{70}$-GNPs in imidazole buffer was incubated in coagulometer cuvettes with prewarmed plasma for 3 minutes, after which clotting was initiated by addition of phospholipid and $CaCl_2$. Tests of the contact pathway of blood clotting were conducted using final concentrations of GNPs as indicated, 33% plasma, 25 μM phospholipid, 1.67 mM imidazole pH 7.0, and 8.33 mM $CaCl_2$.

A_{405} Turbidity Measurements—Turbidity measurements of the same GNPs used above in the coagulometric assays were performed in clear, medium-binding 96-well microplates. A_{405} was typically measured every min for 40–60 min at room temperature (20 °C). Each well contained 50 μl of citrated human pooled normal plasma (George King Biomedical, Overland Park, KS) pre-warmed to 37°C containing 75 μM phospholipid; 50 μl of GNPs or $polyP_{70}$ (BKGP70) in solution in 5 mM imidazole, pH 7.2; and 50 μl of 25 mM $CaCl_2$. GNPs and $polyP_{70}$ were pre-incubated in the citrated plasma on the microplate at 37°C for 3 min before recalcification to ensure FXII activation.

Supplementary Material

Refer to Web version on PubMed Central for supplementary material.

Acknowledgments

We would like to thank Prof. Seungpyo Hong (Biopharmaceutical Sciences, UIC) for providing the Malvern Zetasizer for zeta potential measurements and Dr. Tad Daniel (RRC, UIC) for assisting with TEM imaging.

Funding

The study was sponsored by the US Army Medical Research and Material Command (WQ81XWH-11-2-0021). The U.S. Army Medical Research Acquisition Activity, 820 Chandler Street, Fort Detrick MD 21702-5014 is the awarding and administering acquisition office. The contents of this article do not necessarily reflect the position or the policy of the government, and no official endorsement should be inferred.

References

(1). Brown MRW, and Kornberg A. (2004) Inorganic polyphosphate in the origin and survival of species. Proc. Natl. Acad. Sci. U.S.A. 101, 16085–16087. [PubMed: 15520374]

(2). Morrissey JH, Choi SH, and Smith SA (2012) Polyphosphate: an ancient molecule that links platelets, coagulation, and inflammation. Blood 119, 5972–5979. [PubMed: 22517894]

(3). Kornberg A. (1995) Inorganic Polyphosphate - toward Making a Forgotten Polymer Unforgettable. J. Bacteriol. 177, 491–496. [PubMed: 7836277]

(4). Smith SA, Mutch NJ, Baskar D, Rohloff P, Docampo R, and Morrissey JH (2006) Polyphosphate modulates blood coagulation and fibrinolysis. Proc. Natl. Acad. Sci. U.S.A. 103, 903–908. [PubMed: 16410357]

(5). Smith SA, and Morrissey JH (2008) Polyphosphate enhances fibrin clot structure. Blood 112, 2810–2816. [PubMed: 18544683]

(6). Smith SA, Choi SH, Davis-Harrison R, Huyck J, Boettcher J, Reinstra CM, and Morrissey JH (2010) Polyphosphate exerts differential effects on blood clotting, depending on polymer size. Blood 116, 4353–4359. [PubMed: 20709905]

(7). Choi SH, Smith SA, and Morrissey JH (2011) Polyphosphate is a cofactor for the activation of factor XI by thrombin. Blood 118, 6963–6970. [PubMed: 21976677]

(8). Han KY, Hong BS, Yoon YJ, Yoon CM, Kim YK, Kwon YG, and Gho YS (2007) Polyphosphate blocks tumour metastasis via anti-angiogenic activity. Biochem. J. 406, 49–55. [PubMed: 17492939]

(9). Rashid MH, Rumbaugh K, Passador L, Davies DG, Hamood AN, Iglewski BH, and Kornberg A. (2000) Polyphosphate kinase is essential for biofilm development, quorum sensing, and virulence of Pseudomonas aeruginosa. Proc. Natl. Acad. Sci. U.S.A. 97, 9636–9641. [PubMed: 10931957]

(10). Keasling JD (1997) Regulation of intracellular toxic metals and other cations by hydrolysis of polyphosphate. Ann. N.Y. Acad. Sci. 829, 242–249. [PubMed: 9472324]

(11). Reusch RN, and Sadoff HL (1988) Putative Structure and Functions of a Poly-Beta-Hydroxybutyrate Calcium Polyphosphate Channel in Bacterial Plasma-Membranes. Proc. Natl. Acad. Sci. U.S.A. 85, 4176–4180. [PubMed: 2454464]

(12). Gezelius K. (1974) Inorganic polyphosphates and enzymes of polyphosphate metabolism in the cellular slime mold Dictyostelium discoideum. Arch. Microbiol. 98, 311–29. [PubMed: 4367840]

(13). Zhang H, Gomez-Garcia MR, Brown MR, and Kornberg A. (2005) Inorganic polyphosphate in Dictyostelium discoideum: influence on development, sporulation, and predation. Proc. Natl. Acad. Sci. U.S.A. 102, 2731–5. [PubMed: 15701689]

(14). Noegel A, and Gotschlich EC (1983) Isolation of a High Molecular-Weight Polyphosphate from Neisseria-Gonorrhoeae. J. Exp. Med. 157, 2049–2060. [PubMed: 6406640]

(15). Docampo R, and Moreno SNJ (1999) Acidocalcisome: A novel Ca2+ storage compartment in trypanosomatids and apicomplexan parasites. Parasitol. Today 15, 443–448. [PubMed: 10511686]

(16). Ruiz FA, Lea CR, Oldfield E, and Docampo R. (2004) Human platelet dense granules contain polyphosphate and are similar to acidocalcisomes of bacteria and unicellular eukaryotes. J. Biol. Chem. 279, 44250–7. [PubMed: 15308650]

(17). Donovan AJ, Kalkowski J, Smith SA, Morrissey JH, and Liu Y. (2014) Size-Controlled Synthesis of Granular Polyphosphate Nanoparticles at Physiologic Salt Concentrations for Blood Clotting. Biomacromolecules 15, 3976–3984 [PubMed: 25268994]

(18). Choi SH, Collins JNR, Smith SA, Davis-Harrison RL, Rienstra CM, and Morrissey JH (2010) Phosphoramidate End Labeling of Inorganic Polyphosphates: Facile Manipulation of Polyphosphate for Investigating and Modulating Its Biological Activities. Biochemistry 49, 9935–9941. [PubMed: 20957999]

(19). Hebbard CFF, Wang Y, Baker CJ, and Morrissey JH (2014) Synthesis and Evaluation of Chromogenic and Fluorogenic Substrates for High-Throughput Detection of Enzymes That Hydrolyze Inorganic Polyphosphate. Biomacromolecules 15, 3190–3196. [PubMed: 25000340]

(20). Renne T. (2010) In Vivo Roles for Factor XII. Blood 116, 1759–1759.

(21). Bock PE, Srinivasan KR, and Shore JD (1981) Activation of Intrinsic Blood-Coagulation by Ellagic Acid - Insoluble Ellagic Acid-Metal Ion Complexes Are the Activating Species. Biochemistry 20, 7258–7266. [PubMed: 6797471]

(22). Heimark RL, Kurachi K, Fujikawa K, and Davie EW (1980) Surface Activation of Blood-Coagulation, Fibrinolysis and Kinin Formation. Nature 286, 456–460. [PubMed: 6447254]

(23). Tans G, Rosing J, and Griffin JH (1983) Sulfatide-Dependent Autoactivation of Human-Blood Coagulation Factor-Xii (Hageman-Factor). J.Biol. Chem. 258, 8215–8222. [PubMed: 6553053]

(24). Smith SA, and Morrissey JH (2008) Heparin is procoagulant in the absence of antithrombin. Thromb. Haemost. 100, 160–162. [PubMed: 18612555]

(25). Griffin JH (1978) Role of Surface in Surface-Dependent Activation of Hageman-Factor (Blood-Coagulation Factor-Xii). Proc. Natl. Acad. Sci. U.S.A. 75, 1998–2002. [PubMed: 273926]

(26). Faxalv L, Boknas N, Strom JO, Tengvall P, Theodorsson E, Ramstrom S, and Lindahl TL (2013) Putting polyphosphates to the test: evidence against platelet-induced activation of factor XII. Blood 122, 3818–3824. [PubMed: 23896408]

(27). Nickel KF, Spronk HM, Mutch NJ, and Renne T. (2013) Time-dependent degradation and tissue factor addition mask the ability of platelet polyphosphates in activating factor XII-mediated coagulation. Blood 122, 3847–3849. [PubMed: 24288413]

(28). Muller F, Mutch NJ, Schenk WA, Smith SA, Esterl L, Spronk HM, Schmidbauer S, Gahl WA, Morrissey JH, and Renne T. (2009) Platelet polyphosphates are proinflammatory and procoagulant mediators in vivo. Cell 139, 1143–1156. [PubMed: 20005807]

(29). Engel R, Brain CM, Paget J, Lionikiene AS, and Mutch NJ (2014) Single-chain factor XII exhibits activity when complexed to polyphosphate. J. Thromb. Haemost. 12, 1513–1522. [PubMed: 25039405]

(30). Haake P, and Koizumi T. (1970) Hydrolysis of phosphinamides and the nature of the P-N bond. Tetrahedron Lett, 4845–4848.

(31). Garrison AW, Boozer CE (1968) The acid-catalized hydrolysis of a series of phosphoroamidates. J. Am. Chem. Soc. 90, 3486–3494.

(32). Mucha A, Grembecka J, Cierpicki T, and Kafarski P. (2003) Hydrolysis of the phosphonamidate bond in phosphono dipeptide analogues - The influence of the nature of the N-terminal functional group. Eur. J. Org. Chem, 4797–4803.

(33). Mucha A, Kunert A, Grembecka J, Pawelczak M, and Kafarski P. (2006) A phosphonamidate containing aromatic N-terminal amino group as inhibitor of leucine aminopeptidase - design, synthesis and stability. Eur. J. Med. Chem. 41, 768–772. [PubMed: 16690170]

(34). Jacobsen NE, and Bartlett PA (1981) A Phosphonamidate Dipeptide Analog as an Inhibitor of Carboxypeptidase-A. J. Am. Chem. Soc. 103, 654–657.

(35). Demers LM, Mirkin CA, Mucic RC, Reynolds RA 3rd, Letsinger RL, Elghanian R, and Viswanadham G. (2000) A fluorescence-based method for determining the surface coverage and hybridization efficiency of thiol-capped oligonucleotides bound to gold thin films and nanoparticles. Anal. Chem. 72, 5535–5541. [PubMed: 11101228]

(36). Corbierre MK, Cameron NS, and Lennox RB (2004) Polymer-stabilized gold nanoparticles with high grafting densities. Langmuir 20, 2867–2873. [PubMed: 15835165]

(37). Liu YL, Shipton MK, Ryan J, Kaufman ED, Franzen S, and Feldheim DL (2007) Synthesis, stability, and cellular internalization of gold nanoparticles containing mixed peptide-poly(ethylene glycol) monolayers. Anal. Chem. 79, 2221–2229. [PubMed: 17288407]

(38). Jackson CM, and Nemerson Y. (1980) Blood-Coagulation. Annu. Rev. Biochem. 49, 765–811. [PubMed: 6996572]

(39). Mandle RJ, Colman RW, and Kaplan AP (1976) Identification of Prekallikrein and High-Molecular-Weight Kininogen as a Complex in Human-Plasma. Proc. Natl. Acad. Sci. U.S.A. 73, 4179–4183. [PubMed: 1069308]

(40). Kushida T, Saha K, Subramani C, Nandwana V, and Rotello VM (2014) Effect of nano-scale curvature on the intrinsic blood coagulation system. Nanoscale 6, 14484–14487. [PubMed: 25341004]

(41). Kim KM, Kim HM, Lee WJ, Lee CW, Kim TI, Lee JK, Jeong J, Paek SM, and Oh JM (2014) Surface treatment of silica nanoparticles for stable and charge-controlled colloidal silica. Int. J. Nanomed. 9, 29–40.

(42). Greenwood R, Lapcikova B, Surynek M, Waters K, and Lapcik L. (2007) The zeta potential of kaolin suspensions measured by electrophoresis and electroacoustics. Chem. Pap. - Chem. Zvesti 61, 83–92.

(43). Margolis J. (1961) The effect of colloidal silica on blood coagulation. Aust. J. Exp. Biol. Med. Sci. 39, 249–258. [PubMed: 13766692]

(44). Zhu S, and Diamond SL (2014) Contact activation of blood coagulation on a defined kaolin/collagen surface in a microfluidic assay. Thromb. Res. 134, 1335–1343. [PubMed: 25303860]

(45). Oslakovic C, Cedervall T, Linse S, and Dahlback B. (2012) Polystyrene nanoparticles affecting blood coagulation. Nanomed.-Nanotechnol. 8, 981–986.

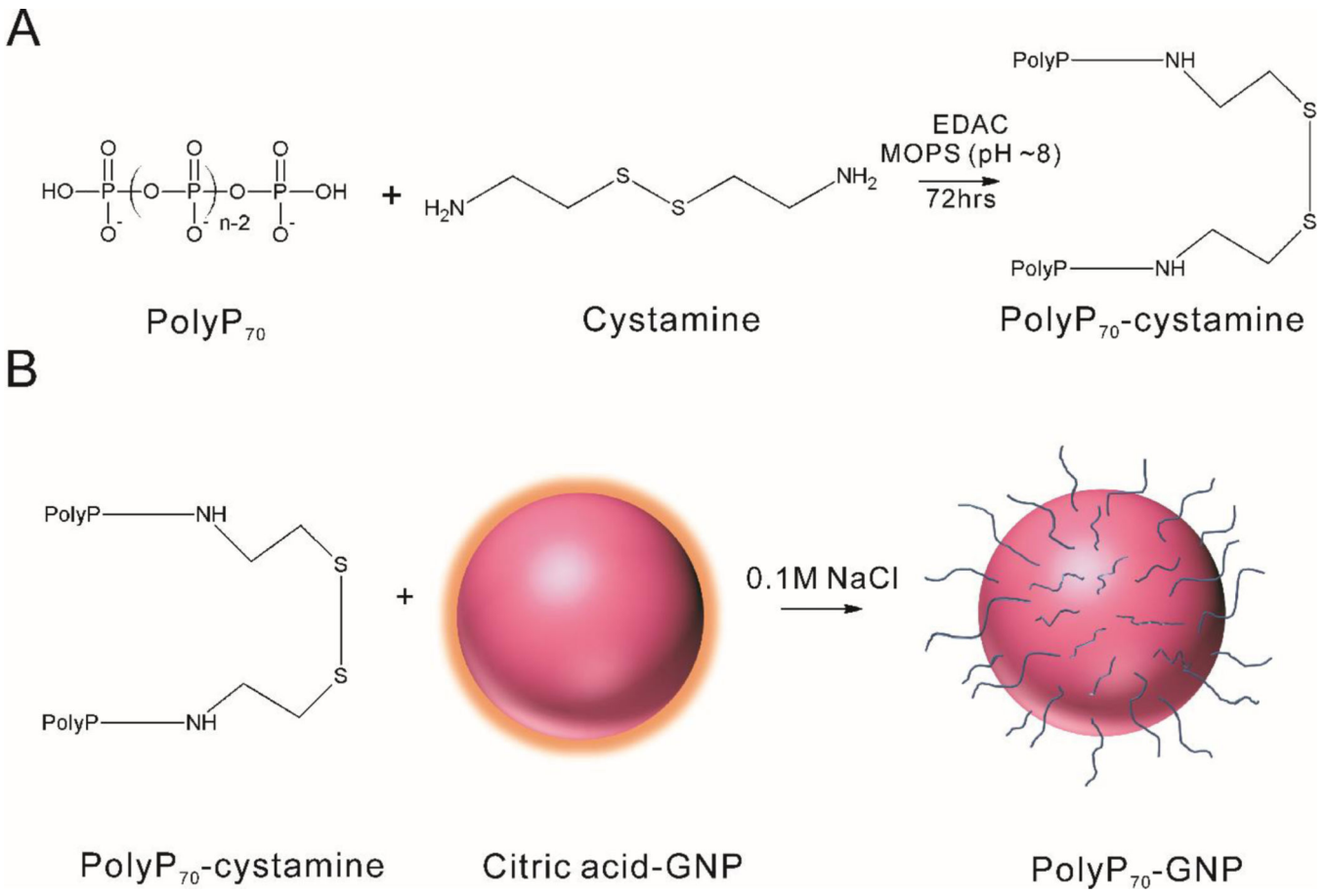

Figure 1. The process of synthesizing GNPs conjugated with polyP$_{70}$.

A: PolyP$_{70}$ is conjugated to cystamine. *B:* PolyP$_{70}$-cystamine is attached to the surface of GNPs.

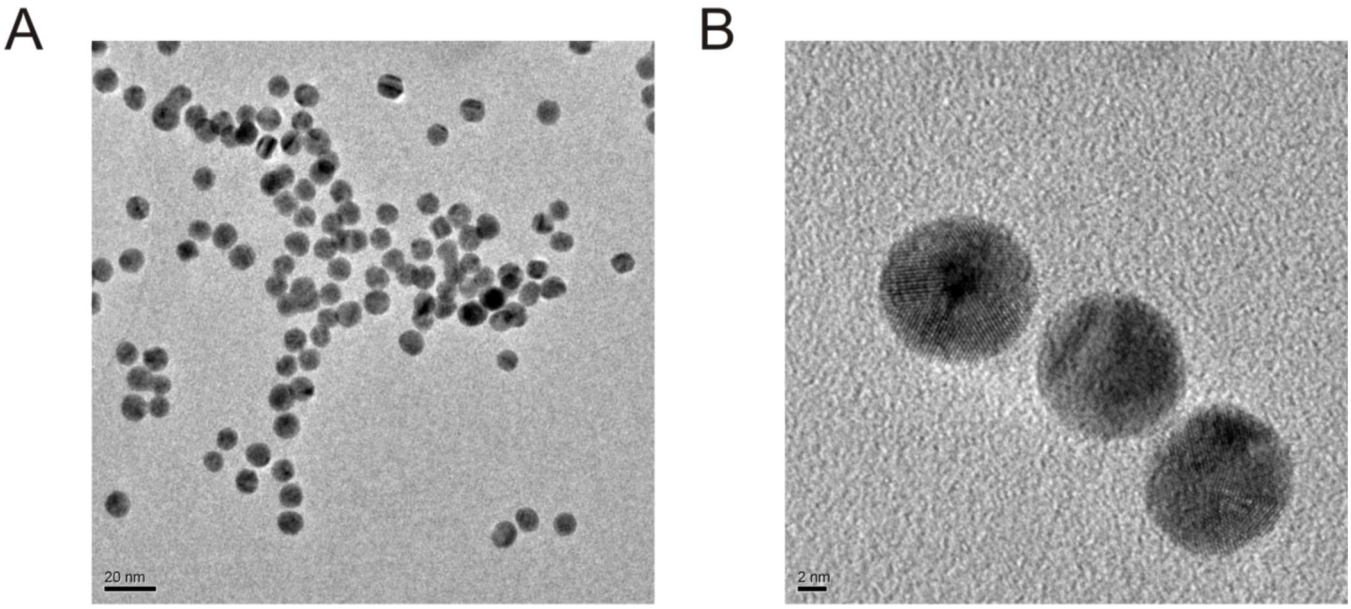

Figure 2. Typical transmission electron micrographs of 10nm polyP$_{70}$-GNPs.

A: polyP$_{70}$-GNPs are spherical and largely free of aggregation several days after synthesis. Scale bar: 20nm. *B*: A trio of polyP$_{70}$-GNPs with the crystal lattices very apparent. Scale bar: 2nm.

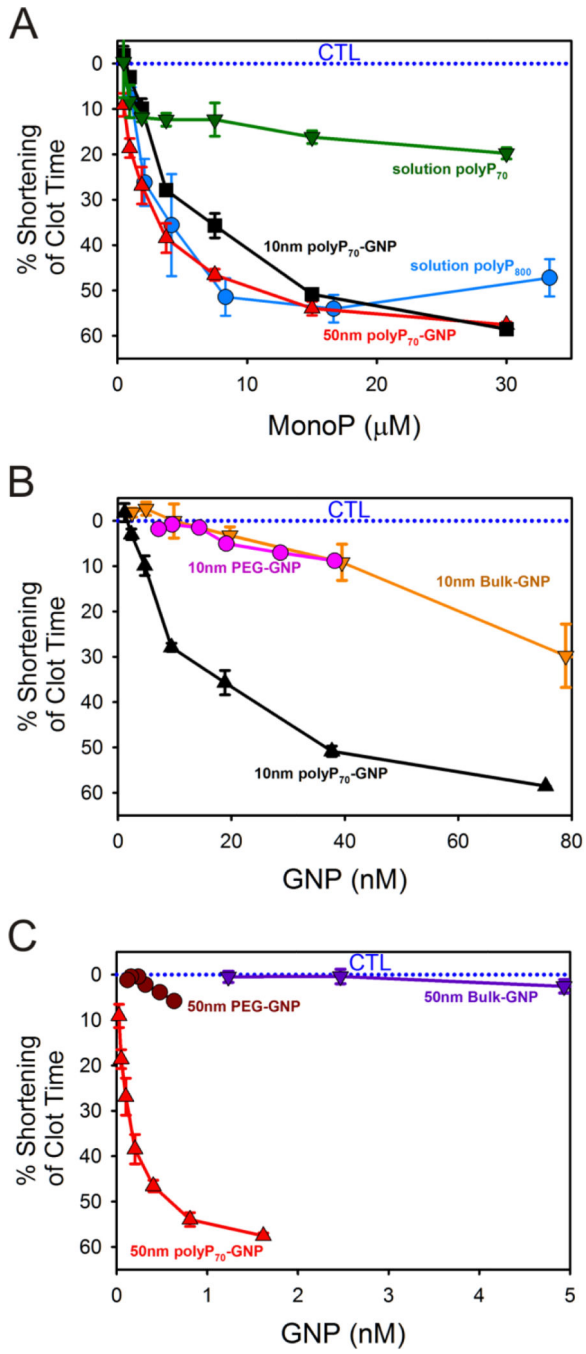

Figure 3. Shortening of clotting time of polyP$_{70}$-GNPs in human plasma when assayed for contact activation as a function of monoP and GNP concentration.

A: Reduction in clotting time of 10nm polyP$_{70}$-GNPs and 50nm polyP$_{70}$-GNPs compared to equivalent concentration of molecularly dissolved polyP$_{70}$ and heterogeneous long-chain polyP$_{800}$. *B*: Reduction of clotting time of 10nm polyP$_{70}$-GNPs compared to the equivalent concentration of 10nm bulk-GNPs and 10nm PEG-GNPs. *C*: Shortenting of clotting time of 50nm polyP$_{70}$-GNPs compared against the same concentration of 50nm bulk-GNPs and 50nm PEG-GNPs.

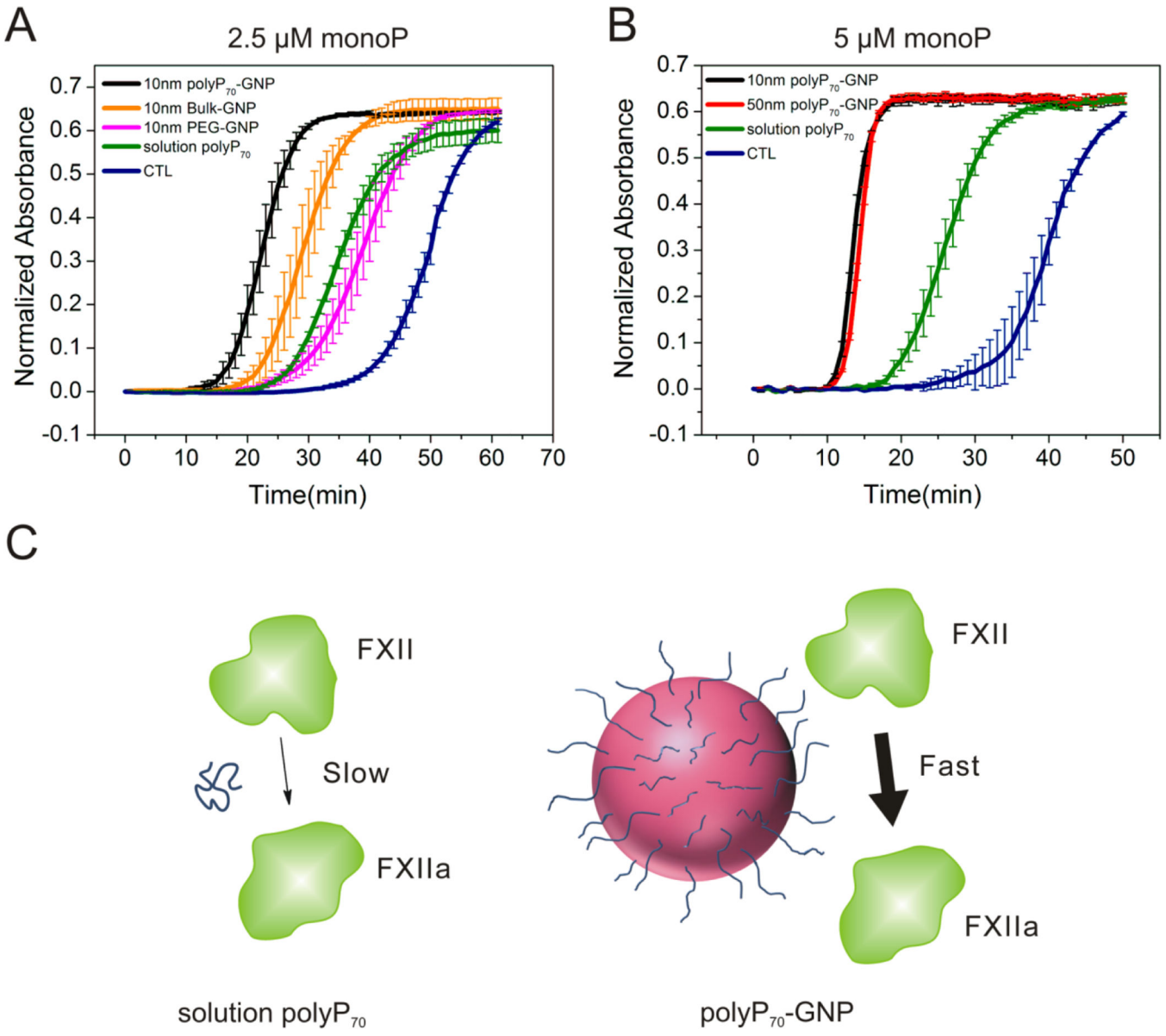

Figure 4. Procoagulant activity of polyP$_{70}$-GNPs assayed by A$_{405}$ turbidity in PNP.

A: Normalized absorbance traces of 10nm polyP$_{70}$-GNPs at 2.5 μM monoP (n=3, ±S.E.) compared to PEGylated GNP and citrate GNP with the same GNP concentration, and molecularly dissolved polyP$_{70}$; *B*: Normalized absorbance traces of 10nm and 50nm polyP$_{70}$-GNPs at 5 μM monoP (n=3, ±S.E.) compared to molecularly dissolved polyP$_{70}$. *C*: **Differential clotting activation of colloidally-anchored and solution-phase polyP$_{70}$.** Colloidal clustering of polyP promotes rapid initiation of the contact pathway of clotting by serving as a surface for the assembly of the primary complex, whereas polyP$_{70}$ in solution is only marginally capable of FXII zymogen activation.

Table 1.

Conjugation efficiency of polyP$_{70}$ and cystamine at various pH conditions.

Buffer	pH of reaction	Efficiency (24 h)	Efficiency (48 h)	Efficiency (72 h)
MOPS (100 mM)	7.1	61.5%	65.0%	71.1%
MOPS (100 mM)	7.6	72.7%	74.3%	78.7%
MOPS (100 mM)	8.1	79.6%	87.3%	88.1%
MOPS (100 mM)	8.5	83.5%	87.3%	88.6%
MES (100 mM)	7.8	81.4%	89.5%	-

Table 2.

Free cystamine concentration (μM) before and after pH adjustment.

pH	Primary amine concentration (μM)				
	Before pH adjustment	**After 1 day**	**After 5 days**	**After 8 days**	**After 13 days**
6.02	16.4 ± 0.49	30.0 ± 0.68	26.4 ± 0.82	27.6 ± 0.17	37.18 ± 1.41
7.07	16.4 ± 0.49	18.6 ± 1.29	14.5 ± 0.31	12.9 ± 0.12	13.72 ± 0.78
9.05	16.4 ± 0.49	17.1 ± 0.85	14.8 ± 0.44	14.2 ± 0.26	15.31 ± 1.36
10.01	16.4 ± 0.49	17.2 ± 0.90	14.8 ± 0.28	12.7 ± 1.2	14.73 ± 0.10

Table 3.

Synthesized $polyP_{70}$-GNPs.

Sample	MonoP conc. (μM)	GNP conc. (nM)	Number of $polyP_{70}$ chains per particle	UV-vis peak for bulk GNP	UV-vis peak after centrifuging
10nm $polyP_{70}$-GNP	90	75.399	17.052	519	521
50nm $polyP_{70}$-GNP	90	1.619	794.195	531	532

Table 4.

ζ Potential measurements of the synthesized samples.

Sample	ζ Potential (mV)
10nm bulk	−19.5
10nm $polyP_{70}$-GNPs	−27.5
10nm PEG-GNP	−3.49
50nm bulk	−22.3
50nm $polyP_{70}$-GNP	−26.53
50nm PEG-GNP	−2.30

Table 5.

Experimental conditions for conjugation of polyP$_{70}$-cystamine to GNPs

GNP size (nm)	GNP starting concentration (nM)	GNP suspension Volume (μl)	Ligand solution (0.1 mM) Volume (μl)	MOPS buffer (pH 8) (μl)
10	9.43	3850	30	120
50	0.374	1970	15	15

Table 6.

Size-dependent centrifugation conditions.

GNP size (nm)	RPM	G-force	Pelleting time (min)	Centrifuge repeat
10	10000	8176	60	3x
50	8000	5223	10	3x